Semantic Web 0 (0) 1
IOS Press

HDT$_{crypt}$: Efficient Compression and Encryption of RDF Datasets

Javier D. Fernández [a,b], Sabrina Kirrane [a], Axel Polleres [a,b] and Simon Steyskal [a,c,*]
[a] *Institute for Information Business, Vienna University of Economics and Business, Austria*
E-mail: {jfernand,sabrina.kirrane,axel.polleres,simon.steyskal}@wu.ac.at
[b] *Complexity Science Hub Vienna, Austria*
[c] *CT RDA BAM CON-AT, Siemens AG, Austria*
E-mail: simon.steyskal@siemens.com

Abstract. The publication and interchange of RDF datasets online has experienced significant growth in recent years, promoted by different but complementary efforts, such as Linked Open Data, the Web of Things and RDF stream processing systems. However, the current Linked Data infrastructure does not cater for the storage and exchange of sensitive or private data. On the one hand, data publishers need means to limit access to confidential data (e.g. health, financial, personal, or other sensitive data). On the other hand, the infrastructure needs to compress RDF graphs in a manner that minimises the amount of data that is both stored and transferred over the wire. In this paper, we demonstrate how HDT – a compressed serialization format for RDF – can be extended to cater for supporting encryption. We propose a number of different graph partitioning strategies and discuss the benefits and tradeoffs of each approach.

Keywords: RDF, HDT, compression, encryption, linked data protection

1. Introduction

In recent years, we have seen an increase in the amount of structured data published online using the Resource Description Framework (RDF), in a manner that not only lends itself to data integration but also supports data interchange. Although Linked Data publishers focus on exposing and linking *open* data, there are scenarios where individuals and organisations need to store and share sensitive or private data. Additionally, there are number of regulations concerning the financial, medical, personal, or otherwise sensitive data that require companies to employ strong data protection mechanisms, such as encryption and anonymisation. In order to ensure confidentially it is necessary to encrypt the data not only when it is *in transit* but also when it is *at rest*. In such scenarios, where multiple users have different access rights to different parts of the data, users should only be able to access the data they are allowed access to.

When it comes to Linked Data protection, to date research has focused on the encryption of partial RDF graphs using eXtensible Markup Language (XML) encryption techniques [19–21] or proposing strategies for querying encrypted RDF data [30]. One of the primary challenges of existing encryption strategies is that they result in a verbose serialization that prevents their use at scale. RDF compression is an emerging research area that focuses on reducing the space requirements of traditional RDF serializations. One approach to efficient data exchange is a (binary) RDF serialization format known as HDT [20] that can be used to compress large datasets in a manner than can be queried without prior decompression [36]. Together encryption and compression mechanisms could be used to cater for the compact storage and efficient exchange of confidential data.

In this paper, we combine "compression+encryption" functionality for RDF datasets, thus allowing service providers to store and share confidential data

*Corresponding author. E-mail: jfernand@wu.ac.at.

while reducing storage and bandwidth usage. In particular, we propose HDT_{crypt}, an extension of HDT to represent encrypted datasets for multiple users with different access rights (i.e. users can only access particular subgraphs of the RDF dataset). To do so, we assume a service provider defines the different "access restricted" subgraphs of a dataset, and we investigate on different partitioning strategies to better capture and represent the redundancy between them in HDT. The contributions of our paper can be summarised as follows, we: (i) demonstrate how HDT compression can be extended to cater for encrypted RDF data; (ii) examine a number of alternative partitioning strategies that can be used to reduce the number of duplicates in encrypted HDT (referred to as HDT_{crypt}); and (iii) compare different partitioning strategies in terms of bandwidth and performance. Experiments show that each of our partitioning strategies are able to achieve space savings over the compression baseline (up to 31%), and are comparable in terms of query performance. We present different space/performance tradeoffs and discuss how partitioning strategies are influenced both by the number of access restricted subgraphs and the distribution of triples across subgraphs.

The rest of the paper is structured as follows: In *Section* 2 we discuss related work on RDF encryption and compression. *Section* 3 provides the necessary background information on HDT and *Section* 4 describes how compression can be combined with encryption. *Section* 5 details the different partitioning strategies that can be used in conjunction with graph based encryption. In *Section* 6 we evaluate using both real-world and synthetic RDF datasets and discusses the trade-off between space and performance. Finally, we conclude and highlight future work in *Section* 7.

2. Related Work

When it comes to encryption and RDF, the focus to date has been on proposing strategies for the partial encryption of RDF graphs [19–21] or the querying of encrypted data [30]. Giereth [20, 21] demonstrate how XML based encryption techniques can be used to encrypt confidential data in an RDF-graph, while all non-confidential data is left as plaintext. Gerbracht [19] built on this work by examining how encryption techniques can be used to encrypt RDF elements and RDF subgraphs, in a manner that minimises the storage overhead. Kasten et al. [30] in turn discuss how data can be encrypted and queried according to SPARQL triple patterns. However this proposal suffers from scalability problems given that each triple is encrypted multiple times depending on whether or not access to the subject, predicate and/or object is restricted. A recent work by Fernández et al. [13] uses Predicate-based Encryption [31] to enable controlled access to encrypted RDF data, i.e., data providers can generate query keys based on (triple-)patterns, whereby one decryption key can decrypt all triples that match its associated triple pattern. In the database and cloud community, Searchable Symmetric Encryption (SSE) [10] has been extensively applied to store and search data in a secure manner. SSE techniques focus on the encryption of outsourced data such that an external user can encrypt their query and subsequently evaluate it against the encrypted data. The more recent Fully Homomorphic Encryption (FHE) [18] technique allows any general circuit/computation over encrypted data, however it is prohibitively slow for most operations [7, 41]. None of these works examine the interplay between encryption and compression, which is the focus of our present paper. In particular, we investigate different HDT compression strategies for RDF datasets, which are organised into different RDF graphs that need to be encrypted with different keys. However, our approach could be adapted to work with partially encrypted graphs.

Following the categorization in [38], an RDF compressor can be classified as either *syntactic* or *semantic*. *Syntactic* compressors try to detect redundancy at the serialisation level, whereas *semantic* compressors try to eliminate logical redundancies. HDT was designed as a binary serialisation format for RDF graphs, but its optimised encodings means that HDT also excels as a syntactic RDF compressor. In HDT RDF data is encoded into two main data-driven components: a *Dictionary* that maps all distinct terms in the dataset to unique identifiers (IDs) (reducing symbolic redundancy), and a triple component that encodes the inner RDF structure as a compact graph of IDs (reducing structural redundancy). This kind of redundancy is also addressed in k^2-triples [1]. However, in the case of k^2-triples the authors perform a predicate-based partition of the dataset into disjoint subsets of (subject, object) pairs. These subsets are highly compressed as (sparse) binary matrices that also allow for efficient data retrieval. RDF compression can also benefit from semantic redundancy. Theoretic foundations of exploiting logical redundancies with respect to rules and grammars have been investigated by [40] and [34], respectively. Likewise, Joshi et al. [28] use rules to dis-

card triples that can be inferred from others, and they only encode these "primitive triples". In doing so they reduce the number of triples and consequently save space. The authors also propose a combination of semantic and syntactic compression, by integrating their approach with syntactic HDT compression techniques. Interestingly the results were similar to those obtained by simply using HDT. Recently, Wu *et al.* [38] have proposed SSP, a hybrid syntactic and semantic compressor. Their evaluation demonstrates that SSP+bzip2 is slightly better than HDT+bzip2. Other approaches, like HDT-FoQ [36] or WaterFowl [9] also enable compressed data to be retrieved without the need for decompression. Both techniques, based on HDT serialization, report competitive performance at the price of using more space than k^2-triples, which to the best of our knowledge, is the most effective compressor. We also use HDT compression, however specifically we examine the syntactic redundancy between RDF graphs that need to be encrypted separately, and propose and evaluate four alternative HDT compression strategies. The exploitation of semantic redundancies within HDT is out of scope and left for future work (for more details on semantic compression and HDT we refer the reader to the work by Hernández-Illera et al. [26]).

3. Preliminaries

Before we present our approach, we need to introduce some concepts and terminology from RDF and HDT. Thereafter, in Section 4, we propose a general mechanism to extend HDT with encryption, termed HDT_{crypt}.

As usual, an *RDF Graph G* is a finite set of triples from $I \cup B \times I \times I \cup B \cup L$, where I, B, L denote IRIs, blank nodes and RDF literals, respectively [24]. Figure 1 shows an example of an RDF graph representing two individuals ex:Bob and ex:Alice, and the project ex:pastProject of the latter. In this paper, we discuss different ways to compress and encrypt such datasets, using HDT a particular compression format for RDF graphs.

HDT [16] is a binary, compressed serialization format for optimized RDF storage and transmission, which also allows certain lookups and queries over compressed data. It is therefore very suitable for the efficient exchange and querying of large datasets. HDT encodes an RDF graph G into three components: the *Header* component H holds metadata, including relevant information necessary for discovery and parsing; the *Dictionary* component D is a catalogue that encodes all RDF terms in G and maps each of them to a unique identifier; the *Triple* component T compactly encodes G's graph structure as tuples of three IDs that are used to represent the directed labelled edges in an RDF graph.

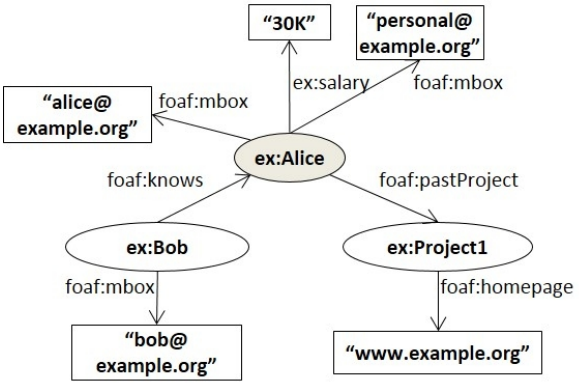

Fig. 1. Example of an RDF graph G.

Figure 2 shows the *Dictionary* component (a), the underlying graph structure (b) and the final *Triple* component (c) for the previous RDF graph G (Figure 1).

3.1. HDT Dictionary Component D

This component organises the terms in a graph G according to their positions in RDF triples, thus we also write $D(G)$ to denote the dictionary component constructed from graph G: the section SO manages terms occurring both as subject and object, and maps them to the ID-range `[1, |SO|]`, where `|SO|` is the number of such terms acting as subject and object. Sections S and O comprise terms that only occur as subjects or objects, respectively. Both sections are mapped from `|SO|+1`, ranging up to `|SO|+|S|` and `|SO|+|S|+|O|`, respectively. Finally, section P organises all predicate terms, which are mapped to the range `[1, |P|]`. It is worth noting that no ambiguity is possible once we know the role played by the corresponding ID. For further details, we refer to [37]. For convenience, we write $id(x, D)$ for the particular ID assigned to an RDF term x, whereas we refer to all IDs and RDF terms mapped in a dictionary component D as $ids(D)$ and $terms(D)$, respectively.

3.2. HDT Triple Component T

This component encodes the *structure* of the RDF graph after ID substitution, taking into consideration

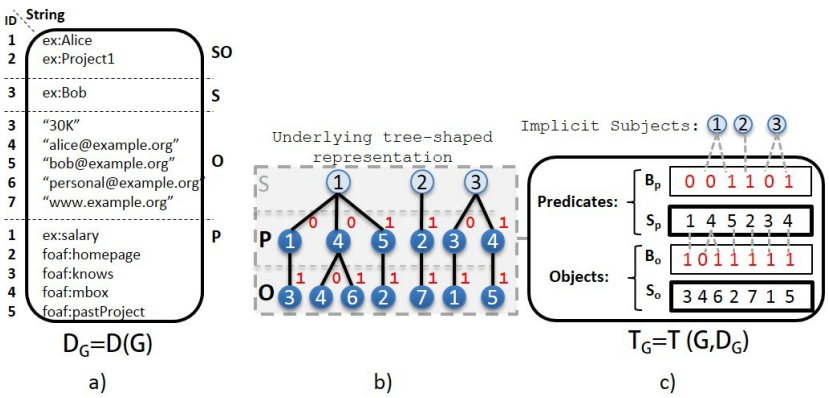

Fig. 2. HDT *Dictionary* and *Triples* for our full graph G.

a particular dictionary D, thus, we write $T(G,D)$ to denote a triple component that was constructed from the triples in G using the IDs in dictionary D. More concretely, RDF triples are encoded as groups of three IDs: $(\mathtt{id}_s\ \mathtt{id}_p\ \mathtt{id}_o)$, where $\mathtt{id}_s$, $\mathtt{id}_p$, and $\mathtt{id}_o$ are the IDs of the corresponding subject, predicate, and object terms in the dictionary. T organises all triples into a forest of trees, one per different subject: the subject is the root; the middle level comprises the ordered list of predicates reachable from the corresponding subject; and the leaves list the object IDs related to each (subject, predicate) pair. This *underlying representation* (illustrated in Figure 2b) is effectively encoded following the *BitmapTriples* approach [16]. It comprises *two sequences*: `Sp` and `So`, concatenating all predicate IDs in the middle level and all object IDs in the leaves, respectively; and *two bitsequences*: `Bp` and `Bo`, which are aligned with `Sp` and `So` respectively, using a 1-bit to mark the end of each list (Figure 2c). Again, we use $ids(T)$ to refer to all IDs used in a triple component T.

3.3. HDT Header Component H

The HDT Header includes (i) the machine-readable metadata that is necessary to process an HDT file (*format metadata*); and (ii) additional human-readable information to describe the dataset (usually in the form of VoID[1] descriptions). The format metadata is mainly focused on characterising the dictionary and triples formats. In general, an HDT file of a graph G consists of a single header H, dictionary dictionary and triples T, $HDT(G) = (H,D,T)$. Nonetheless, the HDT specification [15] is flexible and allows for several dictionaries or triple components to be specified in H as soon as the interpretation of their relationship is provided in the header. It was envisaged that this would be used to split huge RDF graphs into several chunks or streams, where a sequential order of the components is assumed by default [15]. In the following section we exploit and expand this feature to encode a partition of the graph G with several dictionaries and triples.

[1] http://www.w3.org/TR/void/

4. HDT$_{crypt}$: Extending HDT for Encryption

We introduce HDT_{crypt}, an extension of HDT that involves encryption of RDF graphs. We first define the notion of access-restricted RDF datasets and the implications for HDT (Section 4.1). Then, we show an extension of the HDT header component to cope with access-restricted RDF datasets (Section 4.2), which leads to the final HDT_{crypt} encoding. Finally, as HDT_{crypt} can manage several HDT Dictionary components, we describe the required operations to integrate different Dictionary components within an HDT collection (Section 4.3). These operations will be the basis to represent the shared components between access-restricted datasets efficiently, addressed in Section 5.

4.1. Representing access-restricted RDF datasets

We consider hereinafter that users wishing to publish *access-restricted RDF datasets* divide their complete graph of RDF triples G into (named) graphs, that are accessible to other users, i.e. we assume that access rights are already materialised per user group in the form of a set (cover) of separate, possibly overlapping, RDF graphs, each of which are accessible to different sets of users.

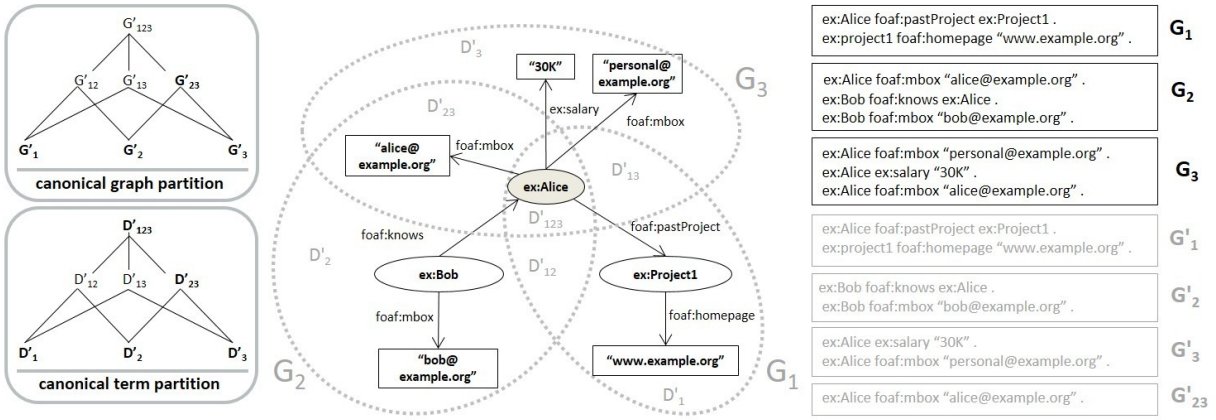

Fig. 3. An access-restricted RDF dataset such that G comprises three separate access-restricted subgraphs G_1, G_2, G_3; the graph's canonical partition is comprised of four non-empty subgraphs $G'_1, G'_2, G'_3, G'_{23}$, whereas the *terms* in these graphs can be partitioned into five non-empty subsets corresponding to the dictionaries $D'_1, D'_2, D'_3, D'_{23}, D'_{123}$.

Borrowing terminology from [25], an *access-restricted RDF dataset* (or just "dataset" in the following) is a set $DS = \{G, (g_1, G_1), \ldots, (g_n, G_n)\}$ consisting of a (non-named) default graph G and named graphs s.t. $g_i \in I$ are graph names, where in our setting we require that $\{G_1, \ldots, G_n\}$ is a cover[2] of G. We further call DS a *partition* of G if $G_i \cap G_j = \emptyset$ for any $i \neq j$; $1 \leqslant i, j \leqslant n$. Note that from any dataset DS, a *canonical partition* DS' can be trivially constructed (but may be exponential in size) consisting of all non-empty (at most $2^n - 1$) subsets $G'_S \in DS'$ of triples $t \in G$ corresponding to an index set $S \in 2^{1,\ldots,i}$ such that $G'_S = \{t \mid t \in \bigcap_{i \in S} G_i \wedge \neg \exists S' : (S' \supset S \wedge t \in \bigcap_{j \in S'} G_j)\}$.

Figure 3 shows an example of such a dataset composed of three access-restricted subgraphs (or just "subgraphs" in the following) G_1, G_2, G_3 for the previous full graph G (Figure 2a). Intuitively, this corresponds to a scenario with three access rights: users who can access general information about projects in an organisation (graph G_1); users who have access to public email accounts and relations between members in the organisation (graph G_2); and finally, users who can view personal information of members, such as the salary and personal email accounts (graph G_3). As can be seen, the triple (ex:Alice foaf:mbox "alice@example.org") is repeated in subgraphs G_2 and G_3, showing a redundancy which can produce significant overheads in realistic scenarios with large-scale datasets and highly overlapping graphs. Canonical partitioning groups these triples into disjoint sets so that no repetitions are present. In our example in Figure 3, the set $G'_{\{2,3\}}$, which can simply be written as G'_{23}, holds this single triple, (ex:Alice foaf:mbox "alice@example.org"), hence this triple is not present in G'_2 and G'_3. In this simple scenario, G'_1 is equivalent to G_1 as it does not share triples with other graphs.

Thus, we consider hereinafter an *HDT collection* corresponding to a dataset DS denoted by $HDT(DS) = (H, \mathcal{D}, \mathcal{T})$ as a single H, plus sets $\mathcal{D} = \{D_1, \ldots, D_n\}$, $\mathcal{T} = \{T_1, \ldots, T_m\}$ of dictionary and triple components, respectively, such that the union of triple components encodes a cover of G, i.e. the overall graph of all triples in the dataset DS. It is worth noting that we do not assume that there is an one-to-one correspondence between individual triple components in $\mathcal{T}$ and graphs in DS; different options of mapping subgraphs to HDT components will be discussed in Section 5 below. The relation between the dictionaries and the triple components (in other words, which dictionaries are used to codify which triple components) is also flexible and must be specified through metadata properties. In our case, we assume $H = \{R, M\}$ to contain a relation $R \subseteq \mathcal{D} \times \mathcal{T}$, which we call the *dictionary-triples map* with the implicit meaning that dictionary components encode terms used in the corresponding triple components, and M is comprised of additional header metadata[3]. It is worth noting that we do not prescribe that either D or T do not overlap. However, it is clear

[2] In the set-theoretic sense.

[3] As mentioned above the header contains a variety of further (meta-)information in standard HDT [15], which we skip for the considerations herein.

that one should find an unambiguous correspondence to decode the terms under $ids(T)$.

Thus, we define the following admissibility condition for R. An HDT collection is called *admissible* if:

- $\forall D_i, D_j \in \mathcal{D} : (D_i, T), (D_j, T) \in R \wedge i \neq j \implies terms(D_i) \cap terms(D_j) = \emptyset$
- $\forall T \in \mathcal{T} : i \in ids(T) \implies \exists (D, T) \in R \wedge i \in ids(D)$

For any admissible HDT collection HDT we define the *T-restricted collection* HDT^T as the collection obtained from removing: (i) all triple components $T' \neq T$ from HDT; (ii) the corresponding D' such that (D', T') is in R and (D', T) is not in R; and (iii) the relations (D', T') from R. Thus allowing an HDT collection to be filtered by erasing all dictionary and triple components that are not required for T.

4.2. HDT_{crypt} encoding

We now introduce the final encoding of the HDT_{crypt} extension. HDT_{crypt} uses AES [11] to encrypt the D and triple components of an HDT collection and extends the header H with a keymap $kmap : \mathcal{D}_{crypt} \cup \mathcal{T}_{crypt} \mapsto I$ that maps *encrypted components* to identifiers (IRIs), which denote AES keys that can be used to decrypt these components. In other words, $HDT_{crypt} = (H, \mathcal{D}_{crypt}, \mathcal{T}_{crypt})$ where $H = \{R, kmap, M\}$, $R \subseteq \mathcal{D}_{crypt} \times \mathcal{T}_{crypt}$, and the components in $\mathcal{D}_{crypt}$ and $\mathcal{T}_{crypt}$ are encrypted with keys identified in $kmap$. We write $encrypt(c, key_{crypt}) = c_{crypt}$, where $c \in \mathcal{D} \cup \mathcal{T}$ to denote the component $c_{crypt} \in \mathcal{D}_{crypt} \cup \mathcal{T}_{crypt}$ obtained by encrypting c with the key key_{crypt}. While, $id(c_{crypt}) \mapsto IRI(key_{crypt})$ is added to the kmap, where id denotes the ID of the component in $\mathcal{D}_{crypt}$ and $\mathcal{T}_{crypt}$ and IRI a unique identifier for the symmetric key. It is assumed that an authorized user u has partial knowledge about these keys, i.e. they have access to a partial function $key_u : I_u \mapsto K$ that maps a finite set of "user-owned" key IDs $I_u \subseteq I$ to the set of AES (symmetric) keys K. We write $decrypt(c_{crypt}, key_{crypt}) = c$, where $c_{crypt} \in \mathcal{D}_{crypt} \cup \mathcal{T}_{crypt}$ to denote the component $c \in \mathcal{D} \cup \mathcal{T}$ obtained from decrypting c_{crypt} with the key $key_{crypt} = key(kmap(c_{crypt}))$. Further we write $decrypt(HDT_{crypt}, I_u)$ to denote the non-encrypted HDT collection consisting of all decrypted dictionary and triple components of HDT_{crypt} which can be decrypted with the keys in $\{key_u(i) \mid i \in I_u\}$. In other words, the T-restriction of HDT_{crypt} is defined analogously to the above-said.

4.3. Integration operations

Finally, we define two different ways of integrating dictionaries $D_1, \ldots, D_k \in \mathcal{D}$ within an HDT collection: *D-union* and *D-merge*. In the former, we replace dictionaries with a new dictionary that includes the union of all terms. In the latter, we establish one of the dictionaries as the dictionary baseline and rename the IDs of the other dictionaries.

4.3.1. D-union

The *D-union* is only defined for $D_1, \ldots, D_k \subseteq \mathcal{D}$ if the following condition holds on R: $\forall (D_i, T) \in R : (\neg \exists D_j \notin D_1, \ldots, D_k$ such that $(D_j, T) \in R)$. In other words, we can perform a D-union if all T-components depending on dictionaries in the set $D_1, \ldots, D_k$ only depend on these dictionaries. Then, we can define a trivial D-union of HDT wrt. $D_1, \ldots, D_k$, written $HDT_{D_1 \cup \ldots \cup D_k}$, as follows:

- replace $\{D_1, \ldots, D_k\}$ dictionaries with a single dictionary $D_{1\ldots k} = D_1 \cup \ldots \cup D_k$, such that $\forall x \in terms(D_1) \cup \ldots \cup terms(D_k)$
  - $x \in terms(D_{1\ldots k})$
  - $id(x, D_{1\ldots k})$ is obtained by sequentially numbering the terms in $terms(D_1) \cup \ldots \cup terms(D_k)$ upon an (arbitrary) total order, e.g., lexicographically ordering the terms (as it is done in HDT dictionaries by default).
- replace all $(D_i, T) \in R$, $i \in \{1, \ldots, k\}$, with new $(D_{1\ldots k}, T')$ relations, where T' is obtained from T by replacing the original IDs from D_i with their corresponding new IDs in $D_{1\ldots k}$.

4.3.2. D-merge

In the more general case where the condition for D-unions does not hold on $D_1, \ldots, D_k \subseteq \mathcal{D}$, we can define another operation, *D-merge*, written $HDT_{D_1 \triangleright \ldots \triangleright D_k}$. We start with the binary case, where only two dictionaries D_1 and D_2 are involved; $HDT_{D_1 \triangleright D_2}$ is obtain as follows:

- replace D_1 and D_2 with a single $D_{12} = D_1 \triangleright D_2$,[4] such that
  - $\forall x \in terms(D_1) : id(x, D_{12}) = id(x, D_1)$
  - $\forall x \in terms(D_2) \setminus terms(D_1) : id(x, D_{12}) = id(x, D_2) + max(ids(D_1))$
- replace all $(D_1, T_1) \in R$ with (D_{12}, T_1)
- replace all $(D_2, T_2) \in R$ with (D_{12}, T_2'), where T_2' is obtained from T_2 by analogous ID changes.

[4] We use the directed operator $\triangleright$ instead of $\cup$ here, since this operation is not commutative.

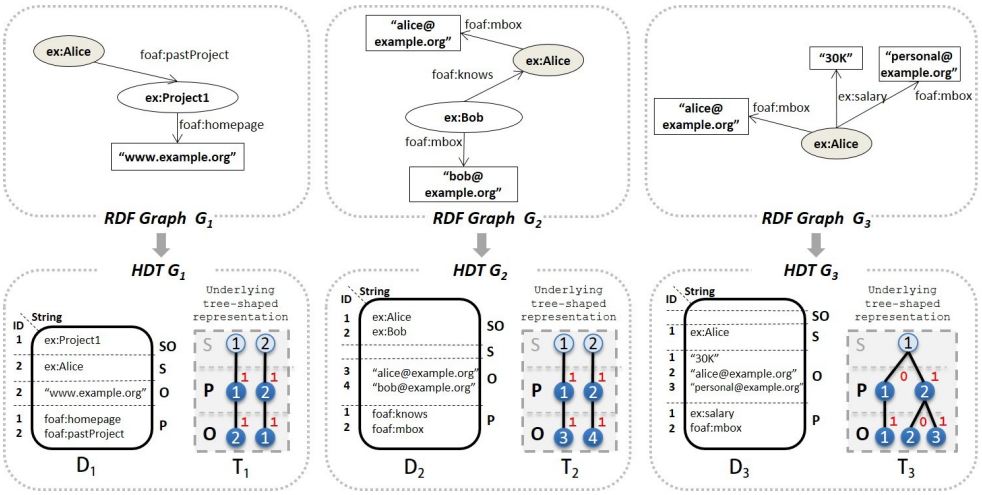

Fig. 4. HDT$_{crypt-A}$, create and encrypt one HDT per partition.

D-merge can then be trivially generalized to a sequence of dictionaries assuming left-associativity of $\triangleright$ operator. That is, $HDT_{D_1 \triangleright D_2 \triangleright \ldots \triangleright D_k} = HDT_{((D_1 \triangleright D_2) \triangleright \ldots) \triangleright D_k}$.

For convenience, we extend the notation of $T(G,D)$ from above to D-unions and D-merges: let $(D_1,\ldots,D_k)$ be a sequence of dictionaries and G an RDF graph such that $terms(G) = \bigcup_{D_i \in (D_1,\ldots,D_k)} terms(D_i)$. Then we will write $T(G,(D_1 \cup \ldots \cup D_k))$ and $T(G,(D_1 \triangleright \ldots \triangleright D_k))$ for the triples part generated from G according to the combined dictionary $((D_1 \cup D_2) \cup \ldots) \cup D_k$ and $((D_1 \triangleright D_2) \triangleright \ldots) \triangleright D_k$ respectively. Finally, we note that for any admissible HDT collection, both D-union and D-merge preserve admissibility.

5. Efficient Partitioning HDT$_{crypt}$

After having introduced the general idea of HDT$_{crypt}$ and the two different ways of integrating dictionaries within an HDT collection, in this section we will discuss four alternatives strategies that can be used to distribute a dataset DS across the dictionary and triple components in an HDT$_{crypt}$ collection, referred to as HDT$_{crypt-A}$, HDT$_{crypt-B}$, HDT$_{crypt-C}$ and HDT$_{crypt-D}$. These alternatives provide different space/performance tradeoffs that will be evaluated in Section 6. We note that HDT behaves differently than the normal RDF merge regarding blank nodes in different "partitions", as there is no standardizing apart taking place [27]: the original blank nodes are skolemized to constants (unique per RDF graph) and preserved across partitions, so that we do not need to consider blank node (re-)naming separately.

5.1. HDT$_{crypt-A}$: A Dictionary and Triples per Named Graph in DS

The baseline approach is straightforward, we construct separate HDT components $D_i = D(G_i)$ and $T_i = T(G_i,D_i)$ per graph G_i in the dataset, see Figure 4, thereafter each of these components is encrypted with a respective, separate key, identified by a unique IRI $id_i \in I$, i.e., $kmap(D_i) = kmap(T_i) = id_i$ and $R = \{(D_i,T_i) \mid G_i \in DS\}$. For re-obtaining graph G_i a user must only have access to the key corresponding to id_i, and can thereby decrypt D_i and T_i and extract the restricted collection HDT^{T_i}, which corresponds to G_i. Obviously, this approach encodes a lot of overlaps in both dictionary and triples parts: that is, for our running example from Figure 4, the IRI for ex:alice is encoded in each individual D component and the overlapping triples in graphs G_2 and G_3 appear in both T_2 and T_3 respectively (cf., Figure 4).

5.2. HDT$_{crypt-B}$: Extracting non-overlapping Triples in DS$'$

In order to avoid the overlaps in the triple components, a more efficient approach could be to split the graphs in the dataset DS according to their canonical partition DS' and again construct separate (D,T)-pairs for each subset $G'_S \in DS'$, see Figure 5. That is, we create $D'_S = D(G'_S)$ and $T'_S = T(G'_S,D'_S)$ per graph $G'_S \in DS'$, where $S \in 2^{1,\ldots,i}$ denotes the index set corresponding to a (non-empty) subset of DS'. R in turn contains pairs (D'_S,T'_S) and $kmap$ entries for keys identified by I'_S per G'_S used for the encryp-

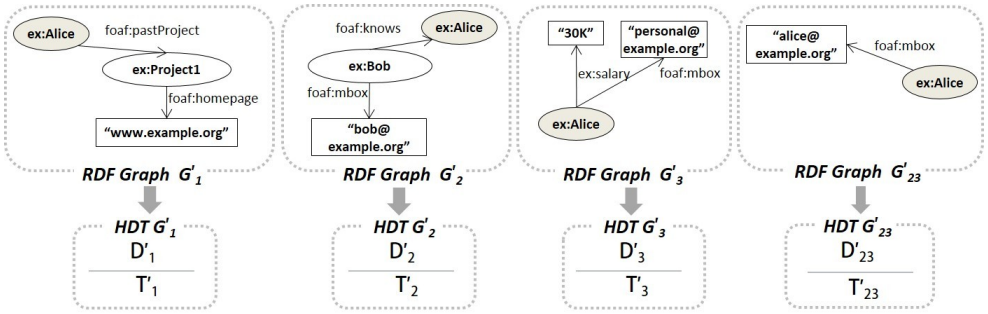

Fig. 5. HDT$_{crypt-B}$, extracting non-overlapping triples.

tion/decryption of the relevant D'_S and T'_S. The difference for decryption now is that any user who is allowed access to G_i must have all keys corresponding to any I'_S such that $i \in S$ in order to re-obtain the original graph G_i. First, the user will decrypt all the components for which they have keys, i.e. obtaining a non-encrypted collection HDT' consisting of components $\mathcal{D}' = \{D'_1, \ldots, D'_k\}, \mathcal{T}' = \{T'_1, \ldots, T'_k\}$ consisting of the components corresponding to a partition of G_i. Then, for decompressing the original graph G_i, we create separate T'_S-restricted $HDT'^{T'_S}$, which are decompressed separately, with G_S being the union of the resulting subgraphs.

5.3. HDT$_{crypt-C}$: Extracting non-overlapping Dictionaries in DS′

Note that in the previous approach, we have duplicates in the dictionary components. An alternative strategy would be to create a *canonical partition* of *terms* instead of triples, and create separate dictionaries $D'_S \in \mathcal{D}'$ for each non-empty term-subset,[5] respectively. Figure 6 shows the canonical partition of terms in our running example: as can be seen, the original dictionary is split into five non-empty terms-subsets corresponding to the dictionaries D'_{123} (terms shared in all three graphs), D'_{23} (terms shared in graphs G_2 and G_3 that are not in D'_{123}) and D'_1, D'_2, D'_3 (terms in either G_1, G_2 or G_3 resp. and are not shared between graphs). This partition can be computed efficiently, thanks to the HDT dictionary D of the full graph G, which we assume to be available[6]. To do so, we keep[7] an auxiliary bitsequence per graph G_i (see Figure 6, top left), each of size $terms(D)$. Then, we iterate through triples in each graph G_i and, for each term, we search its ID in D, marking such position with a 1-bit in the bitsequence of G_i. Finally, the dictionaries of the subsets can be created by inspecting the combinations of 1-bits in the bitsequences: terms in $D'_{xy\cdots z}$ will be those with a 1-bit in the bitsequences of graphs $xy\cdots z$ and 0-bits in other graphs. For instance, in Figure 6, D'_{123} is constituted only by ex:alice, because it is the only term with three 1-bits in the bitsequences of G_1, G_2 and G_3. In contrast, ex:Project1 will be part of D'_1 as it has a 1-bit only in the bitsequence of G_1.

The number of triple components in this approach are as in HDT$_{crypt-A}$, one per graph G_i. However, they are constructed slightly differently as, in this case, we have a canonical partition of terms and one user will just receive the dictionaries corresponding to subsets that correspond to terms in the graph G_i that they have been granted access to. In other words, the IDs used in each T_i should unambiguously correspond to terms, but these terms may be distributed across several dictionaries.[8] Thus, we encode triples with a D-union (see Section 4.3) of the D'_S such that $i \in S$. That is, for each G_i we construct $T_i = T(G_i, (\bigcup_{i \in S} D'_S))$, and add the respective pairs (D'_S, T_i) in R.

Figure 7 illustrates this merge of dictionaries for the graph G_1 and the respective construction of $T(G_1, (D'_1 \cup D'_{123}))$. The decompression process after decryption is the exact opposite. For decompressing the graph G_i, the decrypted dictionaries $\bigcup_{i \in S} D'_S$ are used to create a D-union D_i which can be used to decompress the triples T_i in one go. Finally, as a performance improvement at compression time, note that, although the canonical partition of terms has to be built to be

[5] Again, here $S \in 2^{1,\ldots,n}$ represents an index set.

[6] All HDT$_{crypt}$ strategies are evaluated from an existing full graph G. Our evaluation in Section 6 also reports the time to create the HDT representation of the full graph G

[7] This auxiliary structure is maintained just at compression time and it is not shipped with the encrypted information.

[8] Given the partition definition, it is nonetheless true that a term appears in one and only one term-subset.

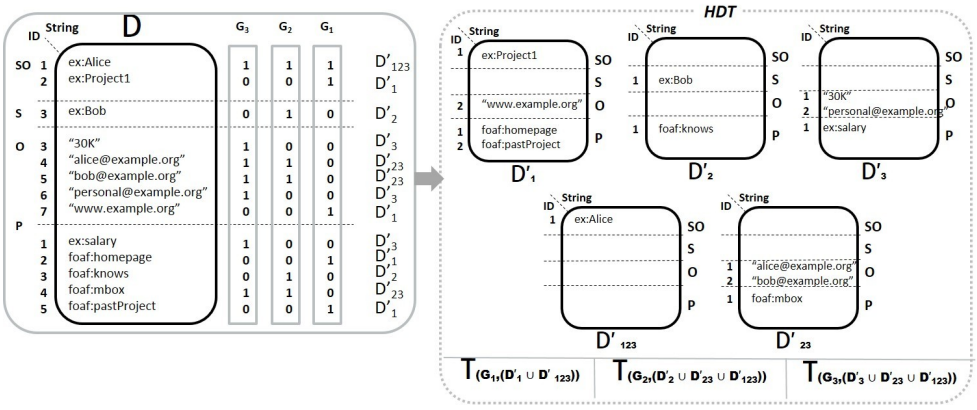

Fig. 6. HDT$_{crypt-C}$, extracting non-overlapping dictionaries.

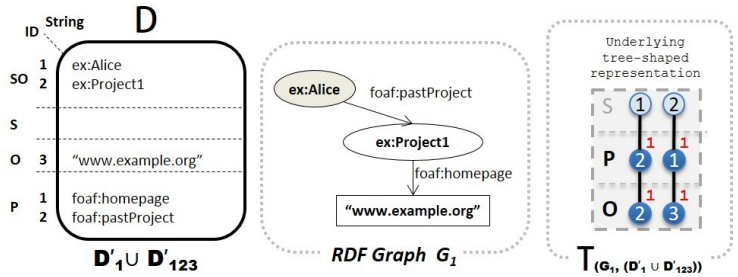

Fig. 7. Union of dictionaries (in HDT$_{crypt-C}$) to codify the non-overlapping dictionaries of a partition.

shipped in the compressed output, we can actually skip the creation of the D-union dictionaries to encode the IDs in the triples. To do so, we make use of the bitsequences to get the final IDs that are used in the triples: One should note that the ID of a term in a D-union of a graph G_i is the number of previous 1-bits in the bitsequence of G_i (for each SO, S, O and P section). For instance, in our example in Figure 7, ex:Project1 is encoded with the ID=2. Instead of creating D_1, we can see that in the bitsequence of G_1 (see Figure 6, top right) we have two 1-bits in the predicate section up to the position where ex:Project1 is stored in the original dictionary, hence its ID=2.

5.4. HDT$_{crypt-D}$: Extracting non-overlapping Dictionaries and Triples in DS'

In HDT$_{crypt-D}$, we combine the methods of HDT$_{crypt-B}$ and HDT$_{crypt-C}$. That is, we first create a *canonical partition of terms* as in HDT$_{crypt-C}$, and a *canonical partition of triples* DS' as in HDT$_{crypt-B}$. Then, we codify the IDs in the subsets of DS' with the IDs from the dictionaries. Note, however, that in this case there is – potentially – an n:m-relation between the resulting dictionary and triple components. In other words, triples in T'_S can include terms that are not only in D'_S as they may be distributed across several term-subsets. For instance, in our running example, T'_1 in HDT$_{crypt-B}$ includes ex:Alice (see Figure 5) which is stored in D'_{123} in HDT$_{crypt-C}$ (see Figure 6). One alternative could be to create a D-union of each graph G'_S and codify triples in T'_S with the corresponding IDs. However, it is trivial to see that this would lead to an exponential number of D-union dictionaries, one per T'_S component. In addition, we would need to physically recreate all these dictionaries at compression time, and also at decompression time in order to decompress each single graph G'_S. Thus, we perform a D-merge approach (see the definition in Section 4.3), which fits perfectly with n:m-relations. This is illustrated in Figure 8. As can be seen, triples in each G'_S of the canonical partition are encoded with an appropriate D-merge of term-subsets. A practical example is shown in Figure 9, representing the encoding of graph G'_3. As defined in D-merge, IDs are assigned in order, that is for a merge

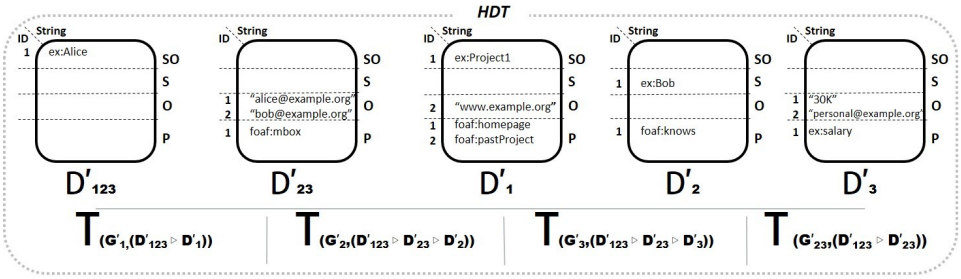

Fig. 8. HDT$_{crypt-D}$, extracting non-overlapping dictionaries and triples.

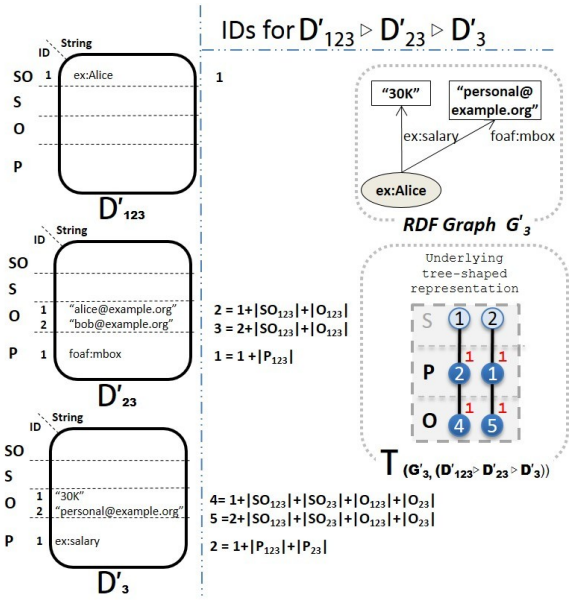

Fig. 9. Merge of dictionaries (in HDT$_{crypt-D}$) to codify the non-overlapping dictionaries and triples of a partition.

$D'_1 \triangleright \ldots \triangleright D'_k$, the IDs in D'_k are shifted $max(ids(D'_1)) + \ldots + max(ids(D'_{k-1}))$. For instance, in our example, the predicate ex:salary will be encoded in G'_3 with the ID=2, because its local ID in D'_3 is 1, and it has to be shifted $max(ids(D'_{123})) + max(ids(D'_{23})) = 1$, hence its final ID= $1+max(ids(D'_{123}))+max(ids(D'_{23})) = 2$. Note that here we restrict the dictionaries D' per section (SO, S, O and P). Given the special numbering of IDs in HDT, where S and O IDs follow from SO as explained in Section 3.1. This is illustrated in our example, e.g. the object "30K" with local ID=1 in D'_3 is mapped in the D-merge dictionary with 4, as it sums up all the previous objects and subjects IDs in D'_{123} and D'_{23}.

It is worth mentioning that no ambiguity is present in the order of the D-merge as it is implicitly given by the partition DS' as per the canonical term partition. Thus, the decompression follows the opposite process: for each graph T'_S in the partition of the graph G_i, the user processes each ID and, depending of the value, they get the associated term in an appropriate term subset. For instance, if the user is accessing the predicate ID=2 in our example, one can easily see that $2 > |P_{123}| + |P_{23}|$, so dictionary D'_3 has to be used[9]. The local ID to look at is then $2 - |P_{123}| - |P_{23}| = 1$, hence the predicate ID=1 in D'_3 is inspected and then foaf:pastProject is retrieved. Finally, note that not all terms in a D-merge are necessarily used when encoding a particular T'_S. For instance, in our example in Figure 9, the object "bob@example.org" with ID=2 in D'_{23} (and ID=3 in the D-merge) is not used in T'_3. However, this ID is "blocked": it cannot be used by a different object in T'_3 as this ID is taken into account when encoding the present objects ("30K" and "personal@example.org"), once we sum the $max(ids(D'_{23}))$ as explained above. The same consequence applies to subjects, so that subject IDs are not necessarily correlative in T'_S. This constitutes a problem for the HDT Bitmap Triples encoding (presented in Section 3.2), given that it represents subjects implicitly assuming that they are correlative. Thus, HDT$_{crypt-D}$ has to explicitly state the ID of each subject, which constitutes a space overhead and a drawback of this approach, despite the fact that duplicate terms and triples are avoided. Technically, instead of a forest of trees, triples are codified as tuples of three IDs, using an existing HDT triples representation called *Plain Triples* [15].

[9] We abuse notation to denote the cardinality of a set, e.g. $|P_{123}|$, as the maximum id represented in such dictionary set.

Table 1
Statistical dataset description

Dataset	Triples	|SO|	|S|	|O|	|P|	Size (GB) NT	NT+lzo	HDT	HDT+gz	HDT creation time (m)
DBpedia	0.43BN	22.0M	2.8M	86.9M	58.3K	61.6	8.6	6.4	2.7	96
LUBM1K	0.13BN	5.0M	16.7M	11.2M	18	18.0	1.3	0.7	0.2	18
LUBM2K	0.27BN	10.0M	33.5M	22.3M	18	36.2	2.7	1.5	0.5	36
LUBM3K	0.40BN	14.9M	50.2M	33.5M	18	54.4	4.0	2.3	0.8	57
LUBM4K	0.53BN	19.9M	67.0M	44.7M	18	72.7	5.3	3.1	1.0	78

6. Evaluation

This section evaluates the performance of HDT$_{crypt}$ by comparing each of the aforementioned partitioning strategies with respect to the performance of the algorithms and the size of the compressed encrypted dataset. We first describe our experimental setup in detail. Then, we present our evaluation results in terms of three distinct yet related tasks: (i) performance of compression and encryption algorithms and size of resulting datasets; (ii) performance of decryption and decompression algorithms; and (iii) performance of triple pattern queries[10] over the compressed datasets, which constitute the basis for SPARQL's graph pattern matching [25]. Finally, we provide a discussion of the results.

6.1. Experimental Setup

The proof-of-concept HDT$_{crypt}$ prototype[11] uses the existing HDT-C++ library[12] for compression and decompression, and standard Java libraries for AES encryption/decryption[13].

The evaluation is performed on two different datasets, a real-world and a synthetic dataset, both of which are described in Table 1. For the real-world dataset we selected DBpedia 3.8, the well-known RDF knowledge base extracted from Wikipedia[14], which was chosen due to the volume and variety of the data and large number of dictionary terms therein. Additionally, in order to test the scalability of the various partitioning strategies we use the Lehigh University Benchmark (LUBM) [23] data generator to obtain synthetic datasets of incremental sizes from 1,000 universities (LUBM1K, including 0.13 billion triples) to 4,000 universities (LUBM4K, 0.53 billion triples). Table 1 shows the original dataset sizes in plain NTriples (NT). In addition, we provide details of the size of the datasets compressed using `lzo`[15], `HDT` and `HDT+gz` (gzip compression over the HDT file). This shows that our HDT compression ratios are in line with the original proposal [16]. Finally, the last column of the table shows the time (in minutes) to compute the HDT representation of each dataset. In turn, the HDT creation time for LUBM grows linearly with the number of triples. This result is also in accordance with the HDT technique, which reports linear scalability regarding the input size and the terms in the dictionary (cf. [16]).

For the LUBM dataset we group data based on the rdf:type of resources and use these groupings to generate three different subgraph datasets (the size of each subgraph is shown in Table 2):

- 12 subgraphs, composed of *UnderGraduateStudent* (G_1), *Courses* (G_2), *Publication* (G_3), *GraduateStudent* (G_4), *Department* (G_5), *ResearchAssistant* (G_6), *AssociateProfessor* (G_7), *TeachingAssistant* (G_8), *FullProfessor* (G_9), *AssistantProfessor* (G_{10}), *University* (G_{11}) and *Lecturer* (G_{12}).
- 9 subgraphs, composed of the union of *UnderGraduateStudent* and *GraduateStudent* (G_1), *Courses* (G_2), *Publication* (G_3), the union of *AssistantProfessor, ResearchAssistant*, and *TeachingAssistant* (G_4), *Department* (G_5), *AssociateProfessor* (G_6), *FullProfessor* (G_7), *University* (G_8) and *Lecturer* (G_9).
- 6 subgraphs, composed of *UnderGraduateStudent* and *GraduateStudent* (G_1), the union of *AssistantProfessor, ResearchAssistant*, *TeachingAssistant*, *Lecturer*, *AssociateProfessor*, *FullProfessor* (G_2), *Courses* (G_3), *Publication* (G_4), *Department* (G_5) and *University* (G_6).

[10] Matching RDF triples in which each component may be a variable

[11] Source code and all experiment data are available at the HDT$_{crypt}$ homepage: https://aic.ai.wu.ac.at/ComCrypt/HDTcrypt/

[12] https://github.com/rdfhdt/hdt-cpp

[13] http://docs.oracle.com/javase/8/docs/technotes/guides/security/crypto/CryptoSpec.html

[14] http://wiki.dbpedia.org/Downloads38

[15] http://www.oberhumer.com/opensource/lzo/

Table 2
% Duplicates and size of subgraphs.

			Size of subgraphs (GB)											
SUBGRAPHS	DATASET	DUP %	G_1	G_2	G_3	G_4	G_5	G_6	G_7	G_8	G_9	G_{10}	G_{11}	G_{12}
6	DBpedia	11.62%	11.6	11.7	11.5	11.7	11.6	11.5						
9	DBpedia	22.32%	8.9	8.9	8.9	8.8	8.9	8.8	8.8	8.9	8.7			
12	DBpedia	32.54%	7.6	7.6	7.7	7.6	7.6	7.6	7.7	7.6	7.6	7.6	7.6	7.5
6	LUBM1K	37.89%	14	5.2	5	4.5	1.6	0.6						
	LUBM2K	37.89%	27	10.7	10.7	8.9	3.1	1.3						
	LUBM3K	37.89%	39.5	16.1	15.2	13.4	4.6	1.9						
	LUBM4K	37.89%	52.8	21.4	20.3	17.9	6.1	2.4						
9	LUBM1K	38.26%	14	5.2	4.5	3.1	1.6	1.3	0.9	0.6	0.2			
	LUBM2K	38.26%	27	10.7	8.9	6.2	3.1	2.3	1.9	1.3	0.4			
	LUBM3K	38.26%	39.5	16.1	13.4	9.2	4.6	3.4	2.8	1.9	0.6			
	LUBM4K	38.26%	52.8	21.4	17.9	13.0	6.1	4.6	3.7	2.4	0.8			
12	LUBM1K	38.10%	8.8	5.1	4.5	4.3	1.5	1.3	1.1	1.1	0.9	0.7	0.6	0.2
	LUBM2K	38.10%	17.7	10.1	8.9	8.6	3.1	2.5	2.3	2.1	1.9	1.5	1.3	0.4
	LUBM3K	38.10%	26.6	15.2	13.4	12.9	4.6	3.8	3.4	3.2	2.8	2.2	1.9	0.6
	LUBM4K	38.10%	35.6	20.3	17.9	17.2	6.1	5.1	4.6	4.2	3.7	3.0	2.4	0.8

When triples represent relations between resources of different types all incoming/outgoing relations are replicated in both subgraphs.

For DBpedia, we generate 6, 9 and 12 subgraphs, each containing randomly selected triples amounting to 10% of the entire corpus (thus ensuring overlaps among subgraphs). Triples that do not appear in any subgraph are subsequently distributed evenly among the subgraphs. Given that the complexity of the partitioning is directly related to the number of duplicates across subgraphs, the size of each of the subgraphs and the overall duplicate ratio, as $\frac{(totalTriples-UniqTriples)}{totalTriples}$, is presented in column DUP % of Table 2. Note that the type-based selection of subgraphs in LUBM generates a skewed distribution of subgraph sizes but similar duplicate ratio (of approximately 38%) at increasing sizes (LUBM1K to LUBM4K). Thus, the comparison between techniques focuses on the effect of the 6/9/12 subgraphs and the efficiency at large scale. In contrast, the even distribution of DBpedia is reflected in the similar size of its subgraphs. Given that the number of duplicates increase with the number of subgraphs (12%, 22% and 33% for 6/9/12 respectively), the effect of duplicates is also evaluated.

In the following we show the performance results of each of the algorithms (compression and encryption, decryption and decompression, integration and querying). Experiments were performed in a –commodity server– (Intel Xeon E5-2650v2 @ 2.6 GHz, 16 cores, RAM 180 GB, Debian 7.9.). All of the reported (elapsed) times are the average of three independent executions in a cold cache scenario (caches are empty at the start of each process).

6.2. Compression and Encryption

Table 3 shows the compression and encryption times as well as corresponding resulting file sizes[16] of the datasets for different partitioning strategies, whereas Table 4 shows the respective number of resulting dictionary and triple components.

The results show that $\text{HDT}_{crypt-C}$ is both the fastest and also produces the most compact representation (only marginally outperformed in space by $\text{HDT}_{crypt-D}$ in particular LUBM cases). $\text{HDT}_{crypt-C}$ is 39% faster than the baseline approach $\text{HDT}_{crypt-A}$ in DBpedia, and 40% faster in LUBM. In contrast, $\text{HDT}_{crypt-B}$ is the slowest approach with a mean of 60% over the baseline, because it needs to create many dictionaries (e.g. 3836 in DBpedia as shown in Table 4) with overlapping terms. In turn, $\text{HDT}_{crypt-D}$ is highly influenced by the number of dictionary components, due to the additional complexity of creating the resp. triple components from the *D*-merge. Thus, $\text{HDT}_{crypt-D}$ is faster than the baseline in LUBM with 6 or 9 subgraphs, with few components as shown in Table 4, but it shows a worse performance with LUBM 12 subgraphs and DBpedia (a mean of 19% slower).

Note that, as stated in Section 5, the creation of $\text{HDT}_{crypt-B}$, $\text{HDT}_{crypt-C}$ and $\text{HDT}_{crypt-D}$ assumes that the HDT representation of the full graph *G* is already computed[17]. Otherwise, the HDT creation time (re-

[16] Note that encryption produces negligible size overheads on the compressed files.

[17] In fact, HDT is becoming popular to store and serve large datasets by publishers and third parties, and a large portion of datasets in the Linked Open Data cloud is already available in HDT

Table 3
Performance of compression and encryption algorithms.

		Compression Time (minutes)				Encryption Time (seconds)				Size (GB)			
SUBGRAPHS	DATASET	*crypt-A*	*crypt-B*	*crypt-C*	*crypt-D*	*crypt-A*	*crypt-B*	*crypt-C*	*crypt-D*	*crypt-A*	*crypt-B*	*crypt-C*	*crypt-D*
6	DBpedia	102	197	**62**	121	98.17	108.84	**80.85**	91.07	9.64	9.33	**7.43**	8.59
9	DBpedia	117	225	**72**	142	124.65	140.40	**98.24**	125.94	11.64	10.91	**7.92**	8.76
12	DBpedia	131	214	**81**	152	**156.52**	245.16	187.90	221.89	13.87	12.49	**8.49**	8.91
6	LUBM1K	34	41	**21**	33	12.25	11.21	**9.85**	10.94	1.40	1.08	**1.05**	**1.05**
	LUBM2K	78	94	**47**	73	21.88	18.74	**17.95**	18.24	2.86	2.19	**2.15**	2.16
	LUBM3K	125	143	**72**	112	32.24	26.82	**25.72**	26.00	4.35	3.31	**3.28**	3.30
	LUBM4K	169	191	**97**	151	54.56	33.83	**33.17**	33.90	5.65	4.45	**4.41**	4.45
9	LUBM1K	37	42	**21**	36	12.96	11.93	**11.33**	11.89	1.44	1.09	1.06	**1.04**
	LUBM2K	78	88	**45**	73	22.80	19.56	**18.97**	19.98	2.93	2.21	2.17	**2.14**
	LUBM3K	126	144	**71**	114	33.79	28.02	27.61	**27.58**	4.45	3.34	3.31	**3.26**
	LUBM4K	174	194	**98**	158	60.11	35.66	35.53	**35.36**	5.97	4.49	4.44	**4.42**
12	LUBM1K	36	44	**23**	39	12.78	13.48	**12.21**	12.98	1.45	1.11	1.06	**1.05**
	LUBM2K	75	94	**49**	82	23.32	21.62	**20.23**	21.38	2.96	2.25	2.17	**2.15**
	LUBM3K	116	142	**73**	126	33.92	29.03	**28.35**	29.50	4.50	3.41	3.31	**3.26**
	LUBM4K	158	190	**99**	175	60.80	37.85	38.20	**37.36**	6.03	4.56	**4.44**	**4.44**

Table 4
Number of dictionaries/triples in each approach.

		Dictionaries			Triples	
				crypt-C	*crypt-A*	*crypt-B*
SUBGRAPHS	DATASET	*crypt-A*	*crypt-B*	*crypt-D*	*crypt-C*	*crypt-D*
6	DBpedia	6	63	63	6	63
9	DBpedia	9	510	511	9	510
12	DBpedia	12	3836	4095	12	3836
6	LUBM	6	20	23	6	20
9	LUBM	9	39	64	9	39
12	LUBM	12	55	122	12	55

ported in Table 1) should be considered as a once-off overhead. In the worst case (i.e. the conversion is done for the only matter of encrypting a single dataset with a particular number of subgraphs), adding this time would make the $\text{HDT}_{crypt-C}$ perform similarly to the baseline in LUBM. In DBpedia, with a richer dictionary of terms, $\text{HDT}_{crypt-C}$ would be 35-50% slower than the baseline.

Additionally, when compared with the baseline approach $\text{HDT}_{crypt-A}$, $\text{HDT}_{crypt-C}$ achieves a mean of 31% space saving in DBpedia and 26% space saving in LUBM. In general, $\text{HDT}_{crypt-B}$, $\text{HDT}_{crypt-C}$ and $\text{HDT}_{crypt-D}$ benefit from having an increasing number of overlapping dictionaries/triples, hence the DBpedia even distribution produces more space savings. For the same reason, an increasing number of subgraphs leads to more duplicates and space savings w.r.t the baseline, e.g. $\text{HDT}_{crypt-C}$ in LUBM achieves 24%, 26% and 27% savings with 6, 9 and 12 subgraphs respectively. It is worth mentioning that despite the fact that $\text{HDT}_{crypt-D}$ isolates the non-overlapping dictionaries and triples, there is an overhead in the representation as we do not use Bitmap Triples but Plain Triples (as stated in Section 5.4). This is more noticeable in DBpedia with long predicate and object lists.

Encryption times are only a small portion of the publication process, where $\text{HDT}_{crypt-C}$ is generally the fastest approach except for DBpedia with 12 subgraphs for which $\text{HDT}_{crypt-A}$ is the fastest, and for LUBM3K/LUBM4K with 9 subgraphs as well as LUBM4K with 12 subgraphs where $\text{HDT}_{crypt-D}$ is marginally faster. Thus we can conclude that both the number of files that need to be encrypted as well as their respective file sizes influence the overall encryption time. Finally, it is worth noting that – as expected – the performance time of the compression and encryption, as well as the result file sizes show linear growth with increasing LUBM datasets.

thanks to the project LOD Laundromat [3], crawling and serving the HDT conversion of datasets (http://lodlaundromat.org/wardrobe/).

Table 5
Performance of decryption and decompression algorithms for M^6, M^9 and M^{12}, i.e., half of the 6/9/12 subgraphs including the smallest/average/largest subgraphs.

		Decryption Time (seconds)				Decompression Time (minutes)			
SUBGRAPHS	DATASET	*crypt-A*	*crypt-B*	*crypt-C*	*crypt-D*	*crypt-A*	*crypt-B*	*crypt-C*	*crypt-D*
M^6	DBpedia	**61.56**	79.08	64.92	79.80	22	18	**14**	18
M^9	DBpedia	**88.64**	148.52	111.84	129.31	26	22	**17**	25
M^{12}	DBpedia	**93.10**	220.46	195.11	242.85	22	22	**17**	26
M^6	LUBM1K	10.82	11.37	**9.80**	13.74	8	7	**5**	7
	LUBM2K	19.24	22.83	**17.15**	27.62	16	14	**11**	15
	LUBM3K	28.35	31.65	**24.78**	45.14	24	20	**16**	22
	LUBM4K	48.56	43.03	**33.70**	59.46	32	27	**21**	29
M^9	LUBM1K	12.84	13.36	**11.86**	17.52	8	10	**6**	8
	LUBM2K	22.77	24.47	**20.63**	33.15	17	21	**12**	16
	LUBM3K	32.94	37.32	**30.30**	48.95	26	32	**18**	23
	LUBM4K	**48.00**	52.35	51.36	70.12	34	41	**24**	32
M^{12}	LUBM1K	**10.75**	11.54	11.73	15.84	7	6	**5**	7
	LUBM2K	**18.50**	20.30	18.99	30.40	14	13	**10**	14
	LUBM3K	**26.60**	31.08	27.00	45.35	21	19	**15**	20
	LUBM4K	**36.62**	39.48	39.09	66.57	29	25	**19**	27

6.3. Decryption and Decompression

According to our use case scenario we assume that a user has been granted access to more than one named graph, but not the total graph. For a fair comparison, given the skewed size distribution of subgraphs in LUBM (see Table 2), we set up a scenario where the user has been granted access to half of the total subgraphs, including the smallest, average and largest subgraphs. This configuration corresponds to decrypting and decompressing the subgraphs referred to as $M^6 = \{G_1, G_3, G_6\}$, $M^9 = \{G_1, G_2, G_5, G_8, G_9\}$ and $M^{12} = \{G_1, G_2, G_6, G_7, G_{11}, G_{12}\}$ in the case of 6, 9 and 12 subgraphs respectively.

Table 5 shows the time to decrypt and decompress each of the respective subgraphs in the case of DBpedia and LUBM.

Decryption times are almost negligible compared to the decompression time – similar to encryption vs. compression time. Again, the number of files is the dominating factor, hence $\text{HDT}_{crypt-A}$ is the fastest approach regarding decryption.

Regarding decompression, (as per compression) $\text{HDT}_{crypt-C}$ is the fastest approach, achieving a mean of 33% time savings in DBpedia and 30% in LUBM w.r.t the baseline $\text{HDT}_{crypt-A}$. In DBpedia, given the even distribution, having 6 subgraphs is always slightly faster than 9 and 12 subgraphs as the latter generates more duplicates. Regarding the number of graphs in LUBM, 6 and 12 subgraphs behave similarly, while the decompression of 9 subgraphs is slightly slower. Nonetheless, we could verify that the difference between 9 and 12 subgraphs is due to the slightly bigger total file size produced by M^9 in comparison to M^{12}. In turn, the difference between 9 and 6 subgraphs is a consequence of the larger number of generated dictionary/triples between 9 and 6 subgraphs (as shown in Table 4). As per compression, there is a linear increase in performance times with increasing dataset sizes.

6.4. Querying Compressed Data

One of the main advantages of HDT compression is that it is possible to perform SPARQL triple pattern queries directly on the compressed data [36]. Whereas this also holds for approach $\text{HDT}_{crypt-A}$, as it already consists of one file per subgraph, the other approaches presented, $\text{HDT}_{crypt-B}$, $\text{HDT}_{crypt-C}$ and $\text{HDT}_{crypt-D}$, split a subgraph in different dictionary (D) and triple (T) components. For these latter approaches, query resolution can be done by two strategies:

1. *Querying an integrated HDT*: This strategy integrates all the dictionary and triple components of a subgraph into a new HDT (i.e. converting to the baseline $\text{HDT}_{crypt-A}$) which can be then queried.
2. *Local query on each dictionary and triple component*: In this case, the query is performed locally in each dictionary and triple component and the results are then integrated. Note that $\text{HDT}_{crypt-C}$ is not viable for this strategy as it would require to perform the D-union of all the dictionaries in order to search the triples IDs, which is then equivalent to integrating $\text{HDT}_{crypt-C}$ into a new HDT to be queried.

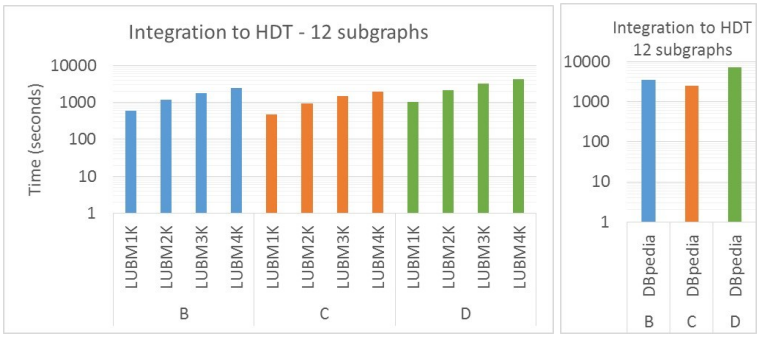

(a) 12 subgraphs (M^{12}) for LUBM (left) and DBpedia (right)

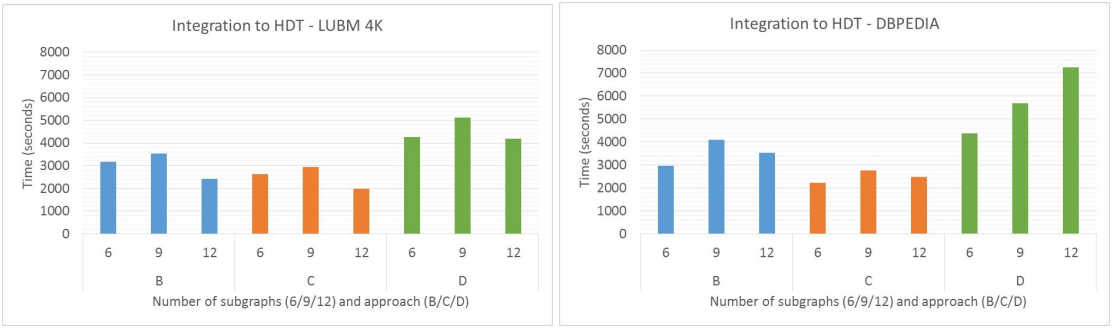

(b) Comparison of 6/9/12 subgraphs (M^6, M^9 and M^{12}) for LUBM4K (left) and DBpedia (right)

Fig. 10. Integration of the dictionary and triple components of M^6, M^9 and M^{12} into one HDT per subgraph.

The following evaluation first inspects the performance overhead of the integration required by the former strategy. Then, we evaluate the query performance of the latter. Note that, although there are a number of strategies for querying *encrypted* data *directly* (see e.g., [4]), we consider these orthogonal and leave combining them with our partitioning for future work.

6.4.1. *Integrating dictionary and triple components into a new HDT*

Following our use case scenario, we assume that a user has decrypted half of the subgraphs, i.e. M^6, M^9 and M^{12} subgraphs. Figure 10 shows the time required by each strategy (i.e. $\text{HDT}_{crypt-B}$, $\text{HDT}_{crypt-C}$ and $\text{HDT}_{crypt-D}$) to integrate their dictionary and triple components into one HDT per subgraph (e.g. G_1, G_2, G_6, G_7, G_{11} and G_{12} for M^{12}), *similarly to* the baseline $\text{HDT}_{crypt-A}$. This integration is performed as follows. First, all dictionary components are fed into a new dictionary, reorganizing the mapping between all terms and their corresponding IDs (as defined in Section 3.1). This first process is similar to the first step of the *D*-union (see Section 4.3.1). Then, we read the triple components and use the new dictionary to convert the triples to the new IDs, integrating all of them in a single new triple component per subgraph[18].

We present the time to integrate the dictionary and triple components of M^{12} into the corresponding subgraphs (Figure 10 a), for both LUBM and DBpedia at increasing sizes. Yet again we see that $\text{HDT}_{crypt-C}$ is the fastest approach, 29% and 56% faster than B and D in DBpedia, and 17% and 44% in LUBM respectively. In general, all approaches shows a linear increase over dataset sizes.

A comparison in terms of number of subgraphs is shown in Figure 10 b, reporting the times of merging M^6, M^9 and M^{12} for LUBM4K (the trends are similar for all LUBM datasets) and DBpedia. As expected, given that the integration process yields to a partial decompression of the dictionary and triple components, the integration performance follows the same pattern as the decompression. That is, in LUBM, 6 is slightly faster than 12 subgraphs (but they behave similarly), while having 9 subgraphs introduced bigger sizes w.r.t. 12, which introduces additional per-

[18]Note that this process slightly differs from the *D*-union as the latter only replaces the new IDs in each of the input triple component.

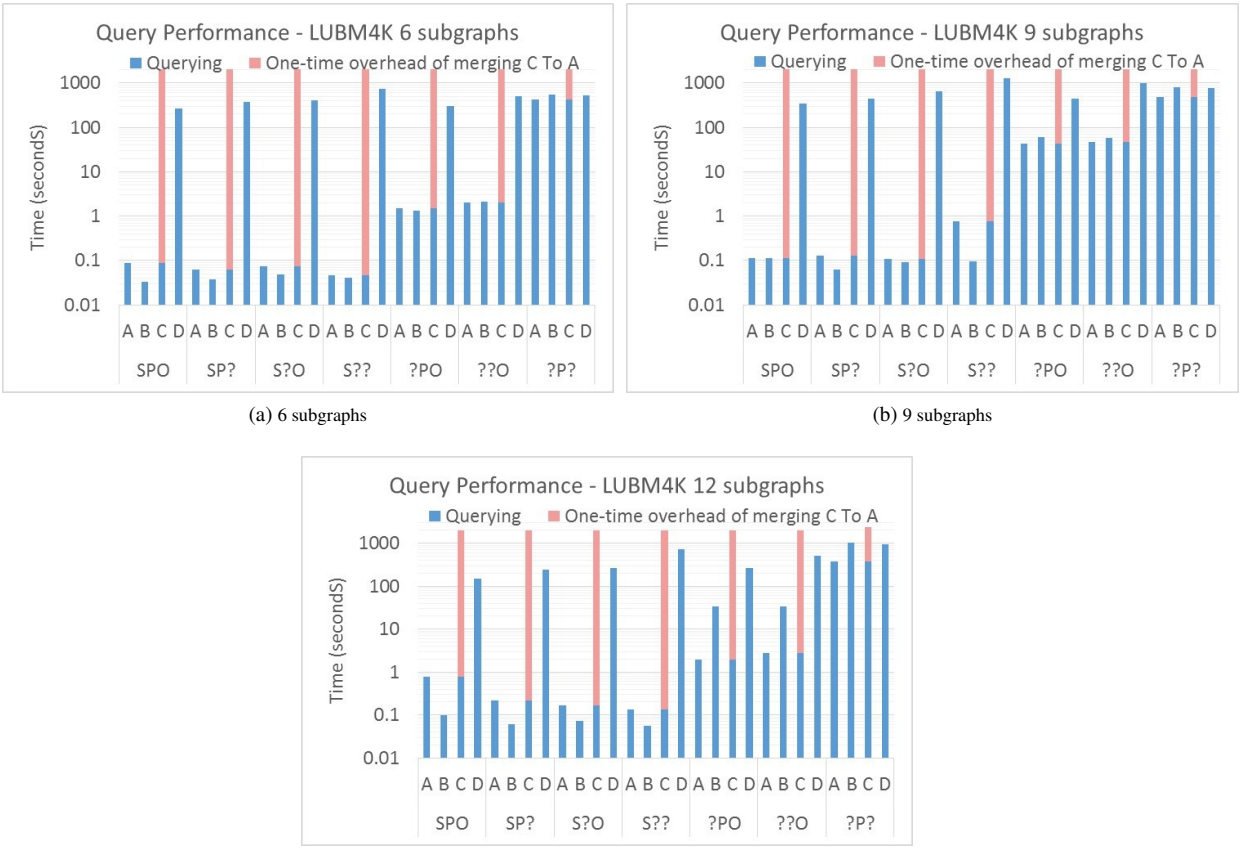

(a) 6 subgraphs

(b) 9 subgraphs

(c) 12 subgraphs

Fig. 11. Performance of Triple Patterns over LUBM4K.

formance overhead. The even distribution of DBpedia results in a faster performance for 6 subgraphs, whereas the excessive duplicates of 12 penalises its performance.

6.4.2. *Query Performance*

We evaluate the query performance of all partitioning strategies in our use case scenario. Thus, for each subgraph in M^6, M^9 and M^{12} (in both LUBM and DBpedia) we first generate 30 random queries for each triple pattern type[19], assuring an even presence of different predicates. Figures 11 and 12 show the execution time of the selected queries for LUBM4K (results for smaller datasets follow the same trends) and DBpedia respectively. Note that, as shown in the previous section, the integration into a new HDT results in a non-negligible time to perform the process. Thus, for $\text{HDT}_{crypt-A}$, $\text{HDT}_{crypt-B}$ and $\text{HDT}_{crypt-D}$ we follow the strategy where queries are executed locally in each dictionary and triple component. In contrast, query execution in $\text{HDT}_{crypt-C}$ would require the D-union of all the dictionaries to be created, which is then equivalent to integrating $\text{HDT}_{crypt-C}$ into a new HDT to be queried. As such, the performance time for $\text{HDT}_{crypt-C}$ is presented as the sum of the time taken to create one integrated HDT (performed once), as previously explained in Section 6.4.1, and to subsequently query the integrated HDT (note again that this latter is equivalent to querying $\text{HDT}_{crypt-A}$).

Regarding the comparison between our strategies for partitioning, results in LUBM (Figure 11) show that $\text{HDT}_{crypt-A}$ and $\text{HDT}_{crypt-B}$ have the best performance for all patterns. This can be attributed to the fact that they benefit from efficient Bitmap Triples indexes, while $\text{HDT}_{crypt-D}$ must use Plain Triples (as stated in Section 5.4) that perform sequential scans to resolve queries. Note that $\text{HDT}_{crypt-D}$ is only competitive in the case of `(?p?)` queries (i.e. retrieving all subjects

[19] All queries are available at the HDTcrypt repository.

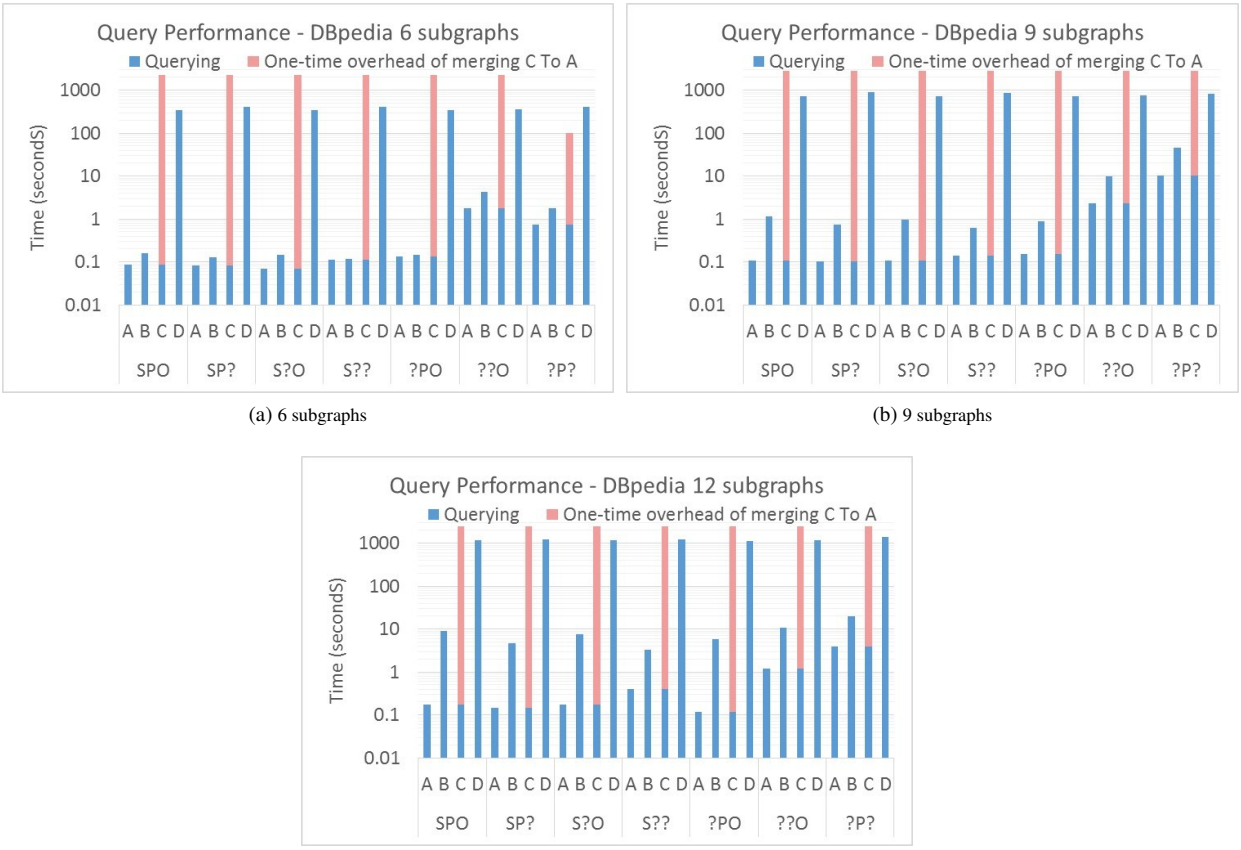

(a) 6 subgraphs

(b) 9 subgraphs

(c) 12 subgraphs

Fig. 12. Performance of Triple Patterns over DBpedia.

and objects related to a given predicate), given that most of the triples are returned and the total time is similar to a full sequential scan. In addition, Bitmap Triples indexes are less efficient for such query types [36].

In turn, it is also worth mentioning that $\text{HDT}_{crypt-B}$ query performance is close to the baseline $\text{HDT}_{crypt-A}$, outperforming its results when few triples are returned, such as `(spo)` and `(sp?)` queries. Note that, although $\text{HDT}_{crypt-B}$ has to query more dictionaries and triple components than $\text{HDT}_{crypt-A}$, the number of total components is very limited in LUBM (the number of components is shown in Table 4) and each component is smaller in $\text{HDT}_{crypt-B}$ than in $\text{HDT}_{crypt-A}$. For instance, the resolution of a `(sp?)` pattern using $\text{HDT}_{crypt-A}$ for M^{12} in LUBM4K (see performance results in Figure 11 a) has to query 6 large triple components (one per subgraph), where duplicated triples can be present. In contrast, for $\text{HDT}_{crypt-B}$ we could verify that there are 37 triple components in M^{12}, but they are smaller and triples do not overlap.

As previously stated, $\text{HDT}_{crypt-C}$ behaves as $\text{HDT}_{crypt-A}$ but there is a once-off overhead associated with merging all dictionary and triple components into one HDT (represented in red in Figure 11).

Although the analysis of results in DBpedia (Figure 12) share most of the previous observations, the differences between methods are more significant. This is mainly due to the larger number of dictionaries/triples to be queried (as shown in Table 4), which penalises the $\text{HDT}_{crypt-B}$ and $\text{HDT}_{crypt-D}$ methods. In this scenario, $\text{HDT}_{crypt-A}$ is the most efficient approach for query execution. The noticeable performance difference against the rest of the partitioning approaches suggests that the once-off merging that is required for $\text{HDT}_{crypt-C}$ can be amortised if the dataset is meant for intensive querying after decryption.

Finally, we design a particular scenario to evaluate the potential influence of the number of graphs in a fair

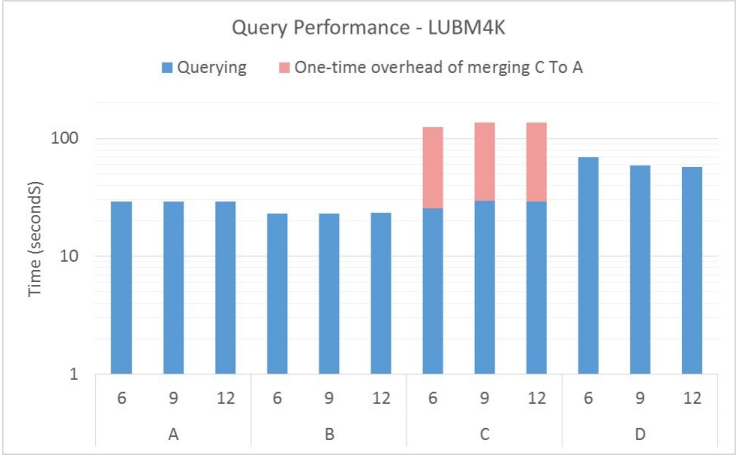

Fig. 13. Performance of all Triple Patterns over LUBM4K in the *University* subgraph.

manner. Note that, in the previous use case, M^6, M^9 and M^{12} include different subgraphs (e.g. *ResearchAssistant* is included as G_6 in M^{12} but it is present neither in M^9 nor M^6). This fact hampers a fair comparison of the query performance, given that the number of results could differ. This situation is even worse in DBpedia, where each subgraph contains randomly selected triples. Thus, for this particular comparison, we select the *University* subgraph in LUBM, which is present in M^{12} (as G_{11} in Table 2), M^9 (as G_8) and M^6 (as G_6). We then generate 30 random triple pattern queries of each type (similarly to the previous scenario) and perform such queries on the aforementioned *University* subgraph. Figure 13 reports the total performance of all queries for LUBM4K (results are similar for smaller sizes). Note that $\text{HDT}_{crypt-A}$ reports the same time in all cases and they compress the same subgraph. In general, results are in line with the previous observations regarding the influence of subgraphs for decompression. That is, in general, 12 subgraphs is the fastest approach, whereas the larger size of the files and their duplication ratio place also a burden on the query performance of 9 subgraphs. Nonetheless, we can find a minor difference in $\text{HDT}_{crypt-D}$, where the case of 6 subgraphs reports the worst performance. A closer look at the generated dictionary and triple components for the particular *University* subgraph allows us to conclude that this particular case produced a skewed distribution of sizes in 6 subgraphs. For example, the largest dictionary component takes 75MB, whereas it is only 27MB and 12MB for 9 and 12 subgraphs respectively. Note that although this skewed distribution is also present in DBpedia, in practice, $\text{HDT}_{crypt-D}$ can be slower with 12 subgraphs than with 6 subgraphs, given that the much larger number of dictionary and triple components in 12 subgraphs (due to the duplication ratio) are the predominant factor.

6.5. Discussion of the results

Overall, our empirical evaluation showed interesting results and allows us to draw conclusions on the applicability of each strategy. We summarize a ranking of results for each scenario in Table 6, and we outline the influence of the increasing number of subgraphs and duplicates in the data in Table 7, detailed as follows:

- $\text{HDT}_{crypt-C}$ is the most effective technique in terms of compression and decompression times, as well as compression sizes. In particular, it achieves additional 26-31% space saving over the –already compressed– baseline ($\text{HDT}_{crypt-A}$), and it is 39-40% faster to compress, and 30-33% faster to decompress. Note that the impact of these space and time savings are even more noticeable when dealing with big data. As we noticed, if the original HDT of the full graph is not available beforehand, then the creation of $\text{HDT}_{crypt-C}$ can take more time than the baseline (it results in approx. the same time in LUBM and 35-50% slower in DBpedia, with a rich dictionary of terms), but it keeps the aforementioned noticeable space savings.
- In contrast, $\text{HDT}_{crypt-C}$ does not allow the user to directly query the exchanged information. If such a scenario is required, this can be solved with a once-off conversion from $\text{HDT}_{crypt-C}$ to $\text{HDT}_{crypt-A}$. This conversion can be done for any

Table 6
Summary of performance of different HDT_{crypt} strategies, where ⋆ ⋆ ⋆ stands for the best performance.

Strategy	Comp. & Encryp.			Decryp. & Decomp.	Querying	
	`Time`	`Size`	`Preconditions`	`Time`	`Time`	`Preconditions`
crypt-A	⋆ ⋆	⋆	*None*	⋆	⋆ ⋆ ⋆	*None*
crypt-B	⋆	⋆ ⋆	HDT of full graph G	⋆ ⋆	⋆ ⋆	*None*
crypt-C	⋆ ⋆ ⋆	⋆ ⋆ ⋆	HDT of full graph G	⋆ ⋆ ⋆	⋆ ⋆	Once-off integration to a new HDT
crypt-D	⋆	⋆ ⋆ ⋆	HDT of full graph G	⋆ ⋆	⋆	*None*

Table 7
Influence of the increasing number of subgraphs and duplicates in the performance of different HDT_{crypt} strategies, where $+++$ stands for very positive and $---$ for very negative.

Strategy	Comp. & Encryp.		Decryp. & Decomp.	Querying
	`Time`	`Size`	`Time`	`Time`
crypt-A	$-$	$-$	$-$	$-$
crypt-B	$-$	$+++$	$-$	$-$
crypt-C	$-$	$+++$	$-$	$-$
crypt-D	$---$	$++$	$-$	$--$

strategy, but it is indeed faster for $\text{HDT}_{crypt-C}$ (17-56% faster than $\text{HDT}_{crypt-B}$ and $\text{HDT}_{crypt-D}$).
– $\text{HDT}_{crypt-B}$ and $\text{HDT}_{crypt-D}$ also reduce the size of the baseline ($\text{HDT}_{crypt-A}$), and can be directly queried. Results show that $\text{HDT}_{crypt-B}$ and $\text{HDT}_{crypt-D}$ gain 6-24% and 24-26% space over the baseline respectively, at the cost of an extra 60% and 19% time for compression (performed only once by the data publisher). In turn, the decompression time outperforms the baseline by 7% and 9% for $\text{HDT}_{crypt-B}$ and $\text{HDT}_{crypt-D}$ respectively.
– The performance of directly querying several subgraphs in $\text{HDT}_{crypt-B}$ is close to the baseline $\text{HDT}_{crypt-A}$. Nonetheless, it is penalised at larger number of partitions (such as 12 in our experiments) and larger number of duplicates (such as our even distribution in DBpedia). $\text{HDT}_{crypt-D}$ suffers from the additional problem of performing sequential scans, and it not competitive but for queries that retrieves large number of results.
– Encryption and decryption times are almost negligible compared to the compression/decompression counterparts.
– Compression sizes, compression and decompression times show linear growth with increasing dataset size.
– In general, an increasing number of subgraphs leads to more duplicates and more space savings of our novel $\text{HDT}_{crypt-B}$, $\text{HDT}_{crypt-C}$ and $\text{HDT}_{crypt-D}$ partitioning approaches over the baseline $\text{HDT}_{crypt-A}$. In turn, less data file sizes result in faster decompression of our novel approaches. In contrast, the compression time is penalised given that more components have to be generated. Our experiments also showed that the number of subgraphs does not have a strong influence on the query performance, but the skewed distribution of sizes and the large number of components (such in DBpedia) can result in slight differences between scenarios.

7. Conclusions and Future Work

To date Linked Data publishers have focused on exposing and linking *open* data, however the Linked Data infrastructure could be extended to cater for the storage and exchange of confidential data. In this paper, we discussed how HDT compression can be extended to cater for RDF datasets which needs to be encrypted. Specifically, we proposed a number of different compression strategies that are compatible and demonstrated the need for careful integration when it comes to compressed encrypted RDF data. From our evaluation we can see that our proposal $\text{HDT}_{crypt-C}$ outperforms the other partitioning strategies both in terms of compression and decompression time, and it also produces the most compact representation, resulting in 26-31% space savings over the –already compressed– baseline. $\text{HDT}_{crypt-B}$ and $\text{HDT}_{crypt-D}$ also reduce the size of the baseline significantly. Whereas, when it comes to querying $\text{HDT}_{crypt-A}$ and $\text{HDT}_{crypt-B}$ outperform $\text{HDT}_{crypt-C}$, which incurs additional overhead as the dictionaries and triples need to be integrated in order to support querying. Additionally, we note that compression, decompression and query performance is influenced both by the number of access restricted sub-

graphs and the distribution of triples across subgraphs, especially in $HDT_{crypt-D}$. In future work, we plan to extend our existing work to cater for querying over encrypted compressed data without the need for decryption.

Acknowledgements

Supported by the Austrian Science Fund (FWF): M1720-G11, the Austrian Research Promotion Agency (FFG) under grant 845638, and European Union's Horizon 2020 research and innovation programme under grant 731601.

References

[1] S. Álvarez-García, N. Brisaboa, J.D. Fernández, M.A. Martínez-Prieto and G. Navarro, Compressed Vertical Partitioning for Efficient RDF Management, *Knowl. Inf. Syst.* **44**(2) (2015), 439–474.

[2] S. Auer, C. Bizer, G. Kobilarov, J. Lehmann, R. Cyganiak and Z. Ives, Dbpedia: A nucleus for a web of open data, in: *Proc. of ISWC*, 2007.

[3] W. Beek, L. Rietveld, H.R. Bazoobandi, J. Wielemaker and S. Schlobach, LOD laundromat: a uniform way of publishing other people's dirty data, in: *Proc. of ISWC*, LNCS, Vol. 8796, Springer, 2014, pp. 213–228.

[4] M. Bellare, A. Boldyreva and A. O'Neill, Deterministic and efficiently searchable encryption, in: *Proc. of CRYPTO*, Springer, 2007, pp. 535–552.

[5] D. Brickley, R.V. Guha and (eds.), RDF Vocabulary Description Language 1.0: RDF Schema, W3C Recomm., W3C, 2004. http://www.w3.org/TR/rdf-schema/.

[6] N. Brisaboa, R. Cánovas, F. Claude, M.A. Martínez-Prieto and G. Navarro, Compressed String Dictionaries, in: *Proc. of SEA*, 2011, pp. 136–147.

[7] M. Chase and E. Shen, Pattern Matching Encryption., *IACR Cryptology ePrint Archive* **2014/638** (2014).

[8] L. Costabello, S. Villata, N. Delaforge and F. Gandon, Linked Data Access Goes Mobile: Context-Aware Authorization for Graph Stores, in: *5th WWW Workshop on Linked Data on the Web*, 2012.

[9] O. Curé, G. Blin, D. Revuz and D.C. Faye, WaterFowl: A Compact, Self-indexed and Inference-Enabled Immutable RDF Store, in: *Proc. of ESWC*, LNCS, Vol. 8465, 2014, pp. 302–316.

[10] R. Curtmola, J. Garay, S. Kamara and R. Ostrovsky, Searchable symmetric encryption: improved definitions and efficient constructions, in: *Proc. of CSS*, ACM, 2006, pp. 79–88.

[11] J. Daemen and V. Rijmen, *The Design of Rijndael: AES - The Advanced Encryption Standard*, Springer, 2013. ISBN 3540425802.

[12] J.D. Fernández, A. Polleres and J. Umbrich, Towards Efficient Archiving of Dynamic Linked Open Data, in: *Proc. of DIACHRON*, 2015.

[13] J.D. Fernández, S. Kirrane, A. Polleres and S. Steyskal, Self-Enforcing Access Control for Encrypted RDF, in: *Proc. of ESWC*, 2017.

[14] J.D. Fernández, Binary RDF for Scalable Publishing, Exchanging and Consumption in the Web of Data, PhD thesis, University of Valladolid, Spain, 2014.

[15] J.D. Fernández, M.A. Martínez-Prieto, C. Gutiérrez and A. Polleres, *Binary RDF Representation for Publication and Exchange (HDT)*, W3C Member Submission, 2011. https://www.w3.org/Submission/HDT/.

[16] J.D. Fernández, M.A. Martínez-Prieto, C. Gutiérrez, A. Polleres and M. Arias, Binary RDF Representation for Publication and Exchange, *J. Web Semant.* **19** (2013), 22–41.

[17] J.D. Fernández, M. Arias, M.A. Martínez-Prieto and C. Gutiérrez, Management of Big Semantic Data, in: *Big Data Computing*, Taylor and Francis/CRC, 2013, Chap. 4.

[18] C. Gentry, Fully homomorphic encryption using ideal lattices., in: *Proc. of STOC*, Vol. 9, ACM, 2009, pp. 169–178.

[19] S. Gerbracht, Possibilities to Encrypt an RDF-Graph, in: *Proc. of ICTTA*, IEEE, 2008, pp. 1–6.

[20] M. Giereth, On Partial Encryption of RDF-Graphs., in: *Proc. of ISWC*, LNCS, Vol. 3729, Springer, 2005, pp. 308–322. ISBN 3-540-29754-5. http://dblp.uni-trier.de/db/conf/semweb/iswc2005.html#Giereth05.

[21] M. Giereth, PRE4J - A Partial RDF Encryption API for Jena, *ACAD MED* **70**(3) (2006), 216–223. http://jena.hpl.hp.com/juc2006/proceedings/giereth/paper.pdf.

[22] J.M. Giménez-García, J.D. Fernández and M.A. Martínez-Prieto, HDT-MR: A Scalable Solution for RDF Compression with HDT and MapReduce, in: *Proc. of ESWC*, 2015, pp. 253–268.

[23] Y. Guo, Z. Pan and J. Heflin, LUBM: A Benchmark for OWL Knowledge Base Systems, *JWS* **3**(2) (2005), 158–182.

[24] C. Gutiérrez, C. Hurtado, A.O. Mendelzon and J. Perez, Foundations of Semantic Web Databases, *JCSS* **77** (2011), 520–541.

[25] S. Harris and A. Seaborne, SPARQL 1.1 Query Language, W3C Recomm., W3C, 2013. http://www.w3.org/TR/sparql11-query/.

[26] A. Hernández-Illera, M.A. Martínez-Prieto and J.D. Fernández, Serializing RDF in compressed space, in: *Data Compression Conference (DCC), 2015*, IEEE, 2015, pp. 363–372.

[27] A. Hogan, M. Arenas, A. Mallea and A. Polleres, Everything You Always Wanted to Know About Blank Nodes, *Journal of Web Semantics (JWS)* (2014), 42–69.

[28] A. Joshi, P. Hitzler and G. Dong, Logical Linked Data Compression, in: *Proc. of ESWC*, LNCS, Vol. 7882, Springer, 2013, pp. 170–184.

[29] L. Kagal, T. Finin and A. Joshi, A Policy Based Approach to Security for the Semantic Web, in: *Proc. of ISWC*, 2003.

[30] A. Kasten, A. Scherp, F. Armknecht and M. Krause, Towards search on encrypted graph data, in: *Proc. of PrivOn'14*, Vol. 1121, CEUR-WS.org, 2013, pp. 46–57.

[31] J. Katz, A. Sahai and B. Waters, Predicate encryption supporting disjunctions, polynomial equations, and inner products, *J. Cryptology* (2013), 1–34.

[32] P. Kolari, L. Ding, G. Shashidhara, A. Joshi, T. Finin and L. Kagal, Enhancing Web Privacy Protection through Declarative Policies, in: *Proc. of POLICY*, 2005.

[33] V. Kolovski, J. Hendler and B. Parsia, Analyzing Web Access Control Policies, in: *Proc. of WWW*, 2007.

[34] S. Maneth and F. Peternek, Grammar-Based Graph Compression, *arXiv preprint arXiv:1704.05254* (2017).

[35] F. Manola and R. Miller, *RDF Primer*, W3C Recomm., 2004, `www.w3.org/TR/rdf-primer/`.

[36] M.A. Martínez-Prieto, M. Arias and J.D. Fernández, Exchange and Consumption of Huge RDF Data, in: *Proc. of ESWC*, LNCS, Vol. 7295, Springer, 2012, pp. 437–452.

[37] M.A. Martínez-Prieto, J.D. Fernández and R. Cánovas, Querying RDF Dictionaries in Compressed Space, *SIGAPP Appl. Comput. Rev.* **12**(2) (2012), 64–77.

[38] J.Z. Pan, J.M. Gómez-Pérez, Y. Ren, H. Wu and M. Zhu, SSP: Compressing RDF data by Summarisation, Serialisation and Predictive Encoding, Technical Report, K-Drive, 2014. http://www.kdrive-project.eu/wp-content/uploads/2014/06/WP3-TR2-2014_SSP.pdf.

[39] S. Pearson and M.C. Mont, Sticky policies: an approach for managing privacy across multiple parties, *Computer* **44**(9) (2011), 60–68.

[40] R. Pichler, A. Polleres, S. Skritek and S. Woltran, Complexity of redundancy detection on RDF graphs in the presence of rules, constraints, and queries, *SWJ* **4**(4) (2013).

[41] R. Popa, N. Zeldovich and H. Balakrishnan, Cryptdb: A Practical Encrypted Relational dbms., Technical Report, MIT-CSAIL-TR-2011-005, 2011. http://hdl.handle.net/1721.1/60876.

[42] E. Rissanen, Extensible access control markup language (xacml) version 3.0, OASIS Standard, available at http://docs.oasis-open.org/xacml/3.0/xacml-3.0-core-spec-en.html, OASIS Committee Specification, 2013.

[43] O. Sacco, A. Passant and S. Decker, An Access Control Framework for the Web of Data, in: *Proc. TrustCom*, 2011, pp. 456–463.

[44] S. Steyskal and S. Kirrane, If you can't enforce it, contract it: Enforceability in Policy-Driven (Linked) Data Markets, in: *Proc. of the Posters and Demos Track SEMANTiCS2015*, 2015.

[45] Q. Tang, On Using Encryption Techniques to Enhance Sticky Policies Enforcement, Technical Report, CTIT University of Twente, 2008. http://eprints.eemcs.utwente.nl/14262/.

[46] H. Van de Sompel, R. Sanderson, M.L. Nelson, L.L. Balakireva, H. Shankar and S. Ainsworth, An HTTP-based versioning mechanism for linked data, in: *Proc. of LDOW*, 2010.